# 2

# Preparation of Nanofluid

## 2.1 Introduction

According to Mahbubul, Elcioglu, Saidur, and Amalina (2017), in order to achieve a "true nano behavior" and to have higher thermal conductivity, stable properties, microchannel cooling without nanoparticle clogging, reduced erosion probability, and reduction of pumping power—in comparison to suspensions of larger particles, nanoparticles should be monodispersed (not agglomerated) within the suspensions (Das, Choi, & Patel, 2006). The stability of nanofluids is of critical importance in this respect (Mahbubul et al., 2017). The performance and capability of nanofluids depend on their dispersion properties, which are related to the preparation method. For practical application of nanofluids, it is necessary that the nanoparticles be uniformly dispersed in fluids to make a stable suspension (Lee et al., 2008). If the nanofluids are not stable, clogging, aggregation, and sedimentation can happen, reducing the performance of suspensions by decreasing thermal conductivity and increasing viscosity. According to Everett (1988), "It is a fundamental principle of thermodynamics that, if a system is kept at a constant temperature, it will tend to change spontaneously in a direction which will lower its free energy. This is exemplified by the simple mechanical case of a weight that falls under the influence of gravity."

Ghadimi, Saidur, and Metselaar (2011) discussed a different aspect of sedimentation with the help of Stokes law (Hiemenz & Rajagopalan, 1997): in a stationary state, the sedimentation velocity of small spherical particles in a liquid follows Eq. (2.1).

$$V = \frac{2R^2}{9\mu}(\rho_P - \rho_L)\, g \tag{2.1}$$

where $V$ is the particle's sedimentation velocity; $R$ is the spherical particle's radius; $\mu$ is the liquid medium viscosity; $\rho_P$ and $\rho_L$ are the particle and the liquid medium density, respectively; and $g$ is the acceleration of gravity. This equation reveals a balance of the gravity, buoyancy force, and viscous drag that are acting on the suspended nanoparticles. According to Eq. (2.1), the following measures can be taken to decrease the speed of nanoparticle sedimentation in nanofluids, and henceforth to produce an improvement for the stability of the nanofluids: (1) reducing $R$, the nanoparticle size; (2) increasing $\mu$, the base fluid viscosity, and (3) lessening the difference of density between the nanoparticles and the base fluid $(\rho_P - \rho_L)$. Clearly reducing the particle size should remarkably decrease the sedimentation speed of the nanoparticles and improve the stability of nanofluids, since $V$ is proportional to the square of $R$. According to the theory of colloid chemistry, when the size of the particle

**Preparation, Characterization, Properties, and Application of Nanofluid. DOI: https://doi.org/10.1016/B978-0-12-813245-6.00002-2**

decreases to a critical size, $R_c$, no sedimentation will take place because of the Brownian motion of nanoparticles (diffusion). However, smaller nanoparticles have a higher surface energy, increasing the possibility of nanoparticle aggregation. Thus, stable nanofluid preparation strongly links up with applying smaller nanoparticles as well as to prevent the aggregation process concurrently (Wu, Zhu, Wang, & Liua, 2009) (this paragraph is adapted from Ghadimi et al. (2011), copyright (2011), with permission from Elsevier).

Preparation of nanofluids is not simply the mixture of solid particles into base fluids. Generally, two techniques have been using to prepare nanofluids: (1) a one-step (single step) method and (2) a two-step (double-step) method.

## 2.2 One-Step Method

When both the manufacturing of nanoparticles as well as the mixture of nanofluid is done in a joint process this is called a one-step method (Eastman, Choi, Li, Yu, & Thompson, 2001; Zhu, Lin, & Yin, 2004). Some commonly used techniques for the one-step method of nanofluid preparation include: direct evaporation method, also called vacuum evaporation onto a running oil substrate (VEROS) technique (Akoh, Tsukasaki, Yatsuya, & Tasaki, 1978; Wagener, Murty, & Günther, 1996), physical vapor deposition (PVD) technique (Eastman et al., 2001), and liquid chemical method (Zhu et al., 2004). The one-step method has both merits and demerits. The most important advantages are the enhanced stability, uniform dispersion, and minimized agglomeration because drying, storage, and transportation of nanoparticles are avoided in this process. The drawbacks of this method are the limited quantity of production due to the slow production process, only low-pressure fluids can be synthesized by this process, and a low concentration of nanoparticles is dispersed in most cases (Mohammed, Al-aswadi, Shuaib, & Saidur, 2011).

### 2.2.1 Physical Method

Some examples of nanofluid preparation by using one-step physical method are described here.

Chang, Jwo, Fan, and Pai (2007) prepared $TiO_2$ nanoparticles and dispersed in water by a one-step physical method. They used ultrasonic-aided submerged arc nanoparticle synthesis system. A schematic of the synthesis system is reprinted in Fig. 2-1. It can be seen in Fig. 2-1 that the setup consists of a few systems (ultrasonic, heating, temperature, and pressure control). Titanium bulk (rod) was used to produce nanoparticles, and is submerged in dielectric liquid (deionized water) in the vacuum chamber. Electrical energy was used as the heat source to generate enough arc with temperatures of 6000−12,000°C, where titanium is melted and vaporized as well as deionized water is also vaporized. A high vapor pressure is created by inertia force of the surrounding deionized water due to the narrow effect and help quick removal of the vaporized metal. Then, the vaporized metal is condensed in the deionized water within the vacuum chamber and forms the $TiO_2$−water nanofluid (Chang et al., 2007; Tsung et al., 2004). The same procedure was used to produce Cu-based

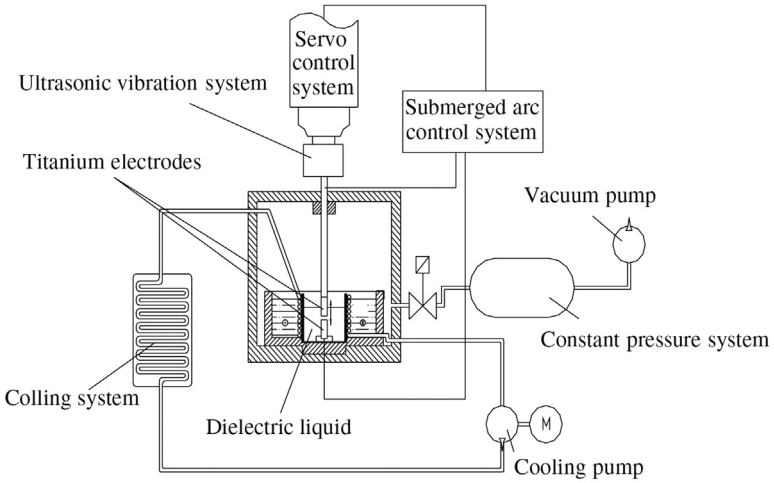


**FIGURE 2-1** Schematic diagram of the ultrasonic-aided submerged arc nanoparticle synthesis system. *Reprinted with permission from Chang, H., Jwo, C.S., Fan, P.S., and Pai, S.H. (2007). Process optimization and material properties for nanofluid manufacturing.* The International Journal of Advanced Manufacturing Technology 34, *300–306. Copyright © 2006, Springer-Verlag London Limited.*

nanofluid in Lo, Tsung, and Chen (2005) and CuO nanofluid in Lo, Tsung, Chen, Su, and Lin (2005). A very similar process was used in Chang and Chang (2008) to produce $Al_2O_3$ nanoparticles where a plasma arc discharge system was used to generate high temperature to vaporize the metal inside the chamber. Such methods are comparatively costly because of the required equipment.

## 2.2.2 Chemical Method

Chemical methods are faster and cheaper in comparison to physical methods. There are different types of chemical methods using by researchers. Some examples are described here.

A pioneering work of a one-step chemical method was introduced by Zhu et al. (2004) to prepare Cu nanofluids of metallic Cu nanoparticles dispersed in ethylene glycol where the reducing agent was $NaH_2PO_2 \cdot H_2O$ and microwave oven was used for heating. The procedure, in short, 25 mL ethylene glycol solution (0.1 M) of copper sulfate pentahydrate ($CuSO4 \cdot 5H_2O$) was mixed with 5 mL of ethylene glycol solution (0.01 M) of polyvinylpyrrolidone (PVP-K30) in a 100-mL beaker, followed by magnetic stirring for 30 min. Then 25 mL of ethylene glycol solution (0.25 M) of sodium hypophosphite ($NaH_2PO_2 \cdot H_2O$) was added and stirred for another 15 min. The mixture was heated at medium power in a microwave oven (700 W, Galanz Microwaves Oven Corp., Shunde, China) to react for 5 min. The color of the mixture turned from blue to dark red after the reaction and Cu nanofluid was acquired when the temperature approached room temperature [this paragraph is adapted from Zhu et al. (2004), copyright (2004), with permission from Elsevier].

Kumar, Meenakshi, Narashimhan, Srikanth, and Arthanareeswaran (2009) synthesized copper−ethylene glycol nanofluids where copper nanoparticles were prepared using sodium hypophosphite as the reducing agent based on the following chemical reactions.

$$2NaH_2PO_2 + 3H_2O + CuSO_4 \rightarrow 2NaH_2PO_3 + H_2SO_4 + 2H_2 + Cu^o \quad (2.2)$$

The procedure was as follows: a 500-mL beaker was used where 25 mL of ethylene glycol (EG) was poured and 15 mL of (0.1 M) copper sulfate pentahydrate, 50 mL of sodium lauryl sulfate (SLS) surfactant, and 100 mL water were added. To avoid oxidation of the prepared nanofluid, a few drops of kerosene were included. A magnetic stirrer/heater was applied for 15 min. Further, 30 mL of sodium hypophosphite was included and the magnetic stirrer was operated for an extra 30 min. The color of the mixture turned from blue to dark red after the reaction. Once the mixture was cooled down and approaching room temperature, Cu nanofluid was collected. A very small amount of dilute sulfuric acid was added to accelerate the reaction. However, the mixture could be neutralized by adding the same quantity of dilute ammonia (Kumar et al., 2009).

Garg et al. (2008) used chemical reduction methods to synthesize Cu nanofluids where 2 g of copper acetate was melted in 50 mL of distilled water with the help of a magnetic stirrer. Then, 0.5 g of sodium hydroxide was included in the mixture and dissolved. The mixture was then cooled down to about 5°C. Then, 3 mL of hydrazine was added, dropwise, to the mixture and the stirrer was continued at room temperature for about 12 h to complete the reduction process. The mixture was centrifuged to separate the Cu particles, which were washed with acetone twice before being vacuum dried at 50°C for 12 h to eliminate water (Garg et al., 2008).

Wei and Wang (2010) synthesized copper nanofluids in a different way using the following chemical reaction:

$$CuSO_4 + 2N_2H_4 \rightarrow Cu + N_2 + 2NH_3 + H_2SO_4 \quad (2.3)$$

The reaction between cupric-sulfate ($CuSO_4$) and hydrazine hydrate ($N_2H_4$) is a classical reduction reaction. Cupric-sulfate ($CuSO_4$) is reduced by hydrazine-hydrate ($N_2H_4$), thus yielding copper (Cu) nanoparticles with $N_2$, $NH_3$, and $H_2SO_4$ as the byproducts. Fig. 2-2 shows the microfluidic system where the chemical reaction takes place. The $CuSO_4$ and $N_2H_4$ fluids are pumped by high-precision syringe pumps (Cole-Parmer Instrument Company, USA) and forced to flow through the microfluidic reactor (Fig. 2-2B). The chemical reaction (2-3) takes place starting from point A where two steams of reactant solutions meet each other. The output channels of the microfluidic reactor allow the nanofluids to vent to the collecting container at atmospheric pressure. The microfluidic reactor consists of a 3-m-long polytetrafluoroethylene (PTFE) micro-bore tubing coil of inner diameter 558 μm (Fig. 2-2C; Cole-Parmer Instrument Company, USA), which is long enough to ensure the completion of reaction (2-3). The micro-bore tubing winds tightly on a cylinder of 2.5 mm in diameter (Fig. 2-2B and D). Two inlets meet at point *A* with a Y-type connector (Cole-Parmer Instrument Company, USA). This microfluidic reactor can have a very rapid mixing

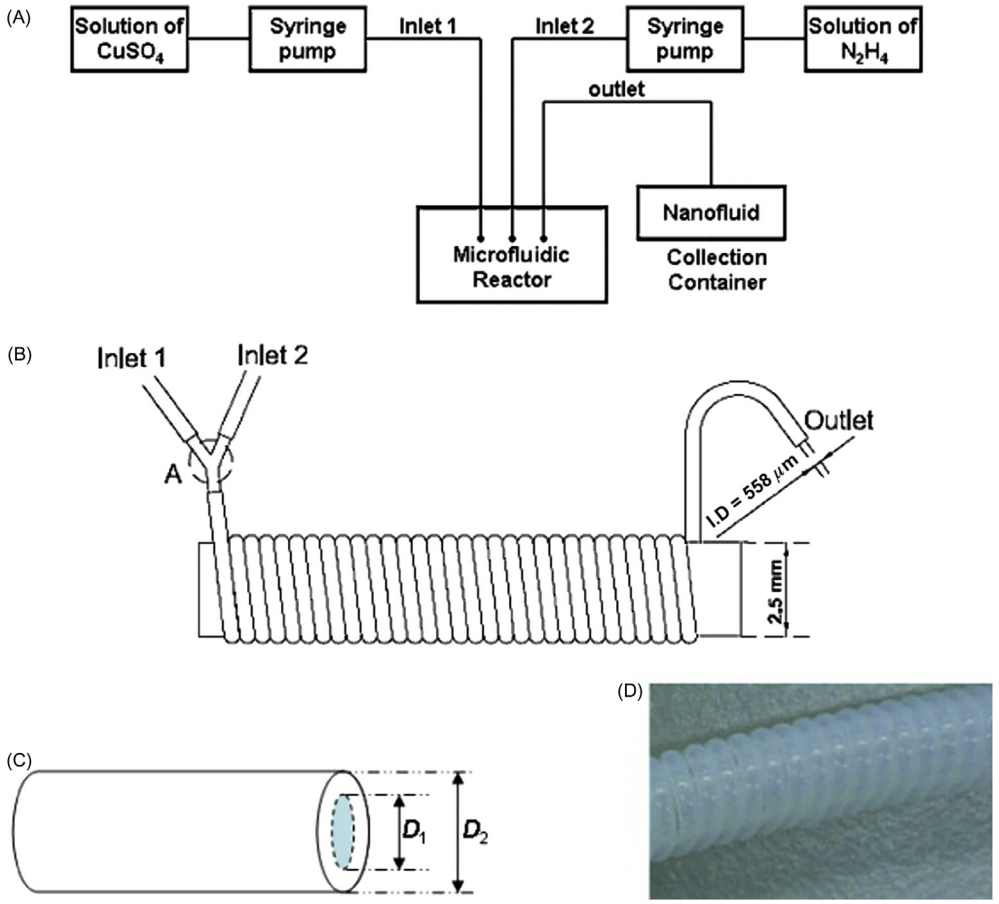


**FIGURE 2-2** Synthesis of microfluidic copper nanofluids: (A) test setup; (B) microfluidic reactor; (C) microbore tube ($D_1 = 558$ μm; $D_2 = 1.0668$ mm); (D) PTFE microbore tubing coil. *Reprinted from Wei, X., and Wang, L. (2010). Synthesis and thermal conductivity of microfluidic copper nanofluids. Particuology* 8, *262–271, copyright (2010), with permission from Chinese Society of Particuology and Institute of Process Engineering, Chinese Academy of Sciences.*

between reactant fluids due to both the short diffusion length and the centrifugal-force-driven transverse secondary flow in curved channels (Wang & Cheng, 1996; Wang & Liu, 2007; Wang & Yang, 2004). By this method, copper nanofluids can be continuously synthesized; their microstructure and properties can be varied by adjusting parameters such as reactant concentration, flow rate, and additive. For the effect of the reactant concentration, the nanofluids are synthesized with a molar concentration of the $N_2H_4$ solution of 0.01, 0.015, and 0.02 M, respectively. The molar concentration of the $CuSO_4$ solution is however fixed at 0.01 M for all three cases of $N_2H_4$ molar concentrations, thus yielding the $CuSO_4/N_2H_4$ molar concentration ratio of 1:1, 1:1.5, and 1:2, respectively. For the effect of flow rate, the $CuSO_4/N_2H_4$ flow rate ratio is set at 1:1 and their flow rate at 10, 20, 30, 40, and

50 μL/min, respectively. The flow rate is precisely controlled and measured by the syringe pump. For the effect of additive, either 5 g/L (mass concentration) polyvinylpyrrolidone (PVP; chemical surfactant) or 30% (volume concentration) glycerol are premixed into both $CuSO_4$ and $N_2H_4$ aqueous solutions. The former can enhance the nanofluid stability and prevent particle aggregation. The latter varies the viscosity of reactant solution and thus affects the reaction environment. (this paragraph is reprinted from (Wei & Wang, 2010), copyright (2010), with permission from Chinese Society of Particuology and Institute of Process Engineering, Chinese Academy of Sciences).

Yu, Xie, Chen, Li, and Zhang (2009) prepared monodispersed copper−water and copper−EG nanofluids by a chemical reduction method. The desired quantity (mentioned in Table 2-1) of PVP and ascorbic acid was dissolved by mechanical stirring in 200 mL of 0.2 mmol/L $CuSO_4$ aqueous (or EG) solution, which was kept at 80°C for some time. Then the mixture was removed from the oil bath and cooled to room temperature. Furthermore, the mixture was diluted in ethanol and centrifuged at 8000 rpm for 15 min to separate Cu particles from the mixture. The separated particles were again suspended in ethanol and centrifuged three times to eliminate surfactant. Finally, the precipitates were dried under vacuum overnight and collected (this paragraph is adapted from Yu et al., 2009). The variation of experimental parameters and results are listed in Table 2-1.

Wei, Zhu, Kong, and Wang (2009) established a chemical solution method (CSM) to produce $Cu_2O$−water nanofluid based on the following chemical reactions in solution:

$$CuSO_4 + 2NaOH = Cu(OH)_2 + Na_2SO_4; \tag{2.4}$$

$$Cu(OH)_2 \triangleq CuO + H_2O; \tag{2.5}$$

$$4CuO + N_2H_4 = 2Cu_2O + N_2 + 2H_2O; \tag{2.6}$$

First, the reaction between cupric-sulfate ($CuSO_4$) and sodium-hydrate (NaOH) forms cupric-hydroxide ($Cu(OH)_2$) and sodium-sulfate ($Na_2SO_4$). Here, NaOH is not only a reagent but also acts to adjust the pH value of the mixture to change particle shape. A constant 40°C

**Table 2-1** Comparison of Results from the Two Reaction Systems and Different Experimental Parameters

| Sample no | Solvent | $CuSO_4$ (mmol/L) | PVP-K30 (mmol/L) | Product | Ascorbic acid/$Cu^{2+}$ (mol/mol) | Reaction Time (h) | Mean Size (nm) |
|---|---|---|---|---|---|---|---|
| 1 | Water | 0.2 | 0.5 | $Cu_2O + Cu$ | 20 | 6 | – |
| 2 | Water | 0.2 | 0.3 | Cu | 20 | 8 | 7 ± 3 |
| 3 | Water | 0.2 | 0.5 | Cu | 20 | 8 | 4 ± 1 |
| 4 | EG | 0.2 | 0.3 | Cu | 8 | 1 | 6 ± 3 |
| 5 | EG | 0.2 | 0.5 | Cu | 8 | 1 | 3 ± 1 |

*Source*: Adapted from Yu, W., Xie, H., Chen, L., Li, Y., and Zhang, C. (2009). Synthesis and Characterization of Monodispersed Copper Colloids in Polar Solvents. Nanoscale Research Letters 4, 465.

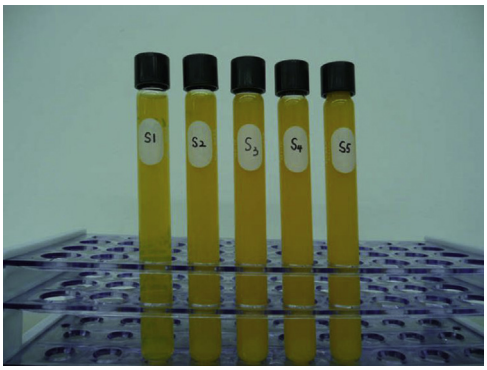


**FIGURE 2-3** Spherical $Cu_2O$ nanofluids 24 h after their preparation ($CuSO_4$ molar concentration from 0.01 to 0.05 mol/L). *Reprinted from Wei, X., Zhu, H., Kong, T., and Wang, L. (2009). Synthesis and thermal conductivity of $Cu_2O$ nanofluids.* International Journal of Heat and Mass Transfer 52*, 4371–4374, copyright (2009), with permission from Elsevier.*

temperature heating by water bath with magnetic stirring, $Cu(OH)_2$ is decomposed into cupric-oxide (CuO) and water ($H_2O$). Then the addition of a reducer as hydrazine-hydrate ($N_2H_4$) reduces CuO to cuprous-oxide ($Cu_2O$). Nitrogen ($N_2$) and water ($H_2O$) are also formed as byproducts. Polyvinylpyrrolidone (PVP) surfactant was used to avoid particle aggregation and to enhance the stability of the suspension (Wei et al., 2009). Fig. 2-3 shows a picture of the synthesized nanofluids with different molar concentration of $CuSO_4$ captured 24 h after preparation.

Patungwasa and Hodak (2008) synthesized gold nanoparticles by modifying the method reported in Enustun and Turkevich (1963). A 1% (w/w) solution of tripotassium citrate (Sigma) is adjusted to the desired pH with 11 M perchloric acid or 3 M NaOH. The citrate solution is first heated to 90°C and quickly (3 s) added to 100 mL of a boiling aqueous solution containing 12 mg of potassium tetrachloroaurate (Aldrich). The temperature was maintained at 100°C with periodic additions of boiling pure water to keep the volume constant. The color of the solution changed from pale yellow to a pale gray before turning into a final color in the brown to red range depending on the pH at which the reaction proceeded. The solution was boiled for 20 min in all cases. The pH of the solution was measured again once the preparation was complete and the temperature of the solution dropped to 25°C. The pH was measured with a Precisa pH 900, immediately after calibration with pH standards at 25°C. All the glassware was cleaned with a 1:1 mixture of concentrated nitric and hydrochloric acids, followed by rinsing with water and cleaned again with a 1:1 mixture of 30% hydrogen peroxide and 98% sulfuric acid (caution: mixtures of hydrogen peroxide and sulfuric acid become very hot and may explode). The glassware was immediately rinsed with copious amounts of deionized water (18.2 MΩ resistivity) and used immediately. The size and shape distributions were evaluated by transmission electron microscopy (TEM) micrographs obtained using formvar-coated 400 mesh copper grids at an accelerating voltage of 30 kV in a Philips H600, or at 80 kV in a Philips TecNAI-G microscope equipped with a CCD camera. Fig. 2-4 shows the TEM micrographs of the nanoparticles prepared at different pHs. The size of the nanoparticles

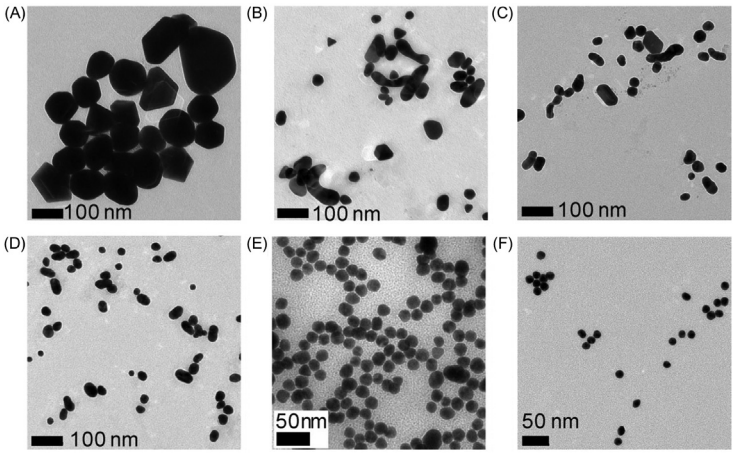


**FIGURE 2-4** Transmission electron micrographs of gold nanoparticles obtained by citrate reduction at the following pH values: (A) 4.0, (B) 4.5, (C) 5.0, (D) 5.5, (E) 6.0, and (F) 6.5. *Reprinted from Patungwasa, W., and Hodak, J.H. (2008). pH tunable morphology of the gold nanoparticles produced by citrate reduction. Materials Chemistry and Physics 108, 45–54, copyright (2007), with permission from Elsevier.*

clearly decreases as the pH is increased, with a noticeable reduction in the size distribution. In addition, crystal faces are more prominent for the nanoparticles obtained with the citrate reduction at pH 4.0 than for those obtained at higher pH values. When the synthesis is carried out at pH 5.0–5.5, a noticeable proportion of nanoparticles tend to have oblate shapes. Other complex shapes are present with larger aspect ratios. This is in contrast to the case in which the reaction was carried out at pH 4.0 or lower. At these pH values, polyhedrons are the prevailing shape and long nanoparticles with smooth surface curvatures are less abundant. As the pH of the citrate solution is increased to 6.5 both the mean as well as the standard deviation of the particle diameter decrease. The spherical-shaped particles are more abundant than the polyhedron or oblate shapes. Nearly spherical nanoparticles are obtained at pH larger than 6.5 but the average diameter stabilizes in the neighborhood of 15 nm. Samples prepared at pH larger than 6.5 yield size distributions with a mean that varies from batch to batch. The standard deviation of the distribution was between 10 and 15% of the mean. When the reduction is carried out at pH lower than 2.0 a large fraction of the gold forms a mirror-like deposit on the glass surface and a very small yield of nanoparticles occurs. For this method, the authors have found that when the pH of the reacting mixture is lower than approximately 3.8 the resulting gold particles no longer stay dispersed after the reaction is complete. The resulting solutions contain dispersions of gold particles visible by eye. The dispersed particles settle down very quickly. [This paragraph is adapted from Patungwasa and Hodak (2008), copyright (2007), with permission from Elsevier.]

Cho, Baek, Lee, and Park (2005) used a chemical reduction method to prepare silver nanoparticles from silver nitrate ($AgNO_3$) and synthesized in ethylene glycol that acted as a solvent and reducing agent. To enhance stability and prevent aggregation of particles poly (acrylamide-*co*-acrylic acid) (PAA-co-AA) stabilizer was used. First, 100 mL of EG was

injected into a flask. Then, various amounts of PAA-co-AA were included and melting in the solvent was controlled at a slower rate to avoid quick entanglement of the stabilizer. The mixture was stirred and swelled enough for 1 h at 120°C. Then, the temperature was controlled at 140°C for 30 min to fully disperse the stabilizer into the solution. After which, $AgNO_3$ was included in the mixture and waited for 60 min more to continue the reaction. Finally, the mixture was cooled down to room temperature (Cho et al., 2005).

## 2.3 Two-Step Method

In a two-step method (Paul, Philip, Raj, Das, & Manna, 2011; Yu, Xie, Li, & Chen, 2011), first, the nanoparticles are primarily arranged and then mixed with the fluid using high shear (Pak & Cho, 1998; Wen & Ding, 2005) or ultrasound (Goharshadi, Ding, Jorabchi, & Nancarrow, 2009) as shown in Fig. 2-5 by a simple diagram. Nowadays, nanoparticles are available from commercial sources. However, due to the high surface energy, it is difficult to avoid aggregation and clustering of nanoparticles. Again, self-weight increase is due to the clustering of particles, which influences rapid sedimentation because of the gravitational effect. This method has attracted scientists and commercial users because of its simplicity. It works well for oxide-based particles. Carbon nanotube nanofluids are also produced by this method but need functionalization or surfactant. The disadvantage of this method is that the particles quickly agglomerate prior to dispersing into the medium and partial dispersion of nanoparticles has also been observed. Table 2-2 shows typical synthesis processes of two-step methods used by the researchers to prepare nanofluids.

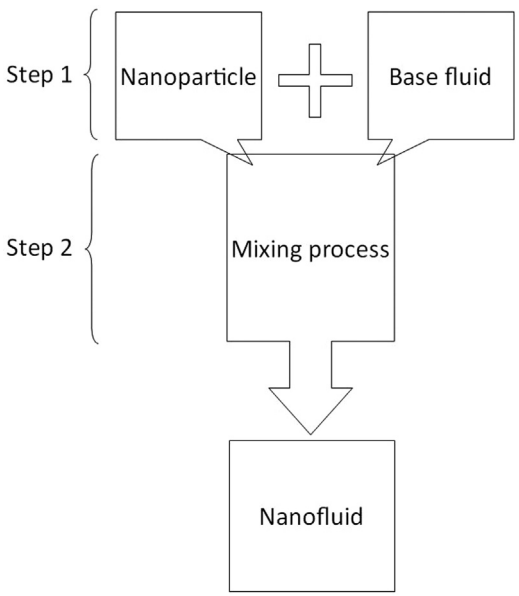


**FIGURE 2-5** Representation of two-step nanofluid preparation method.

**Table 2-2** Summary of Different Types of Synthesis Process Used by the Researchers

| Base Fluid | Nanoparticle (dia. in nm) | Volume (%) | Synthesis Process | References |
|---|---|---|---|---|
| Water | $Al_2O_3$ (37) | 0.01–0.16 | Ball mills | Tseng and Wu (2002) |
| Terpineol | Ni (300) | 3–10 | Ball mills | Tseng and Chen (2003) |
| Water | $TiO_2$ (7–20) | 5–12 | Ball mills | Tseng and Lin (2003) |
| Ethanol | $SiO_2$ (35, 94, and190) | 1.4–7 | Stirring | Chevalier, Tillement, and Ayela (2007) |
| R141b | $Al_2O_3$ (13) | 1–5 | Shaker | Mahbubul (2015) |
| Distilled water | $Al_2O_3$ (13) | 0.5 | Ultrasonic horn | Mahbubul et al. (2014, 2015b), Mahbubul, Saidur, Amalina, and Niza (2016a), Mahbubul, Saidur, Amalina, Elcioglu, and Okutucu-Ozyurt (2015a), Mahbubul, Saidur, Hepbasli, and Amalina (2016b) |
| Distilled water | $TiO_2$ (21) | 0.5 | Ultrasonic horn | Mahbubul et al. (2017) |
| Distilled water, ethylene glycol, engine oil | $Al_2O_3$ (28) | 1–6 | Ultrasonic bath | Wang, Xu, and Choi (1999) |
| Ethylene glycol –water (60:40) | CuO (29) | 0–6.12 | Ultrasonic bath | Namburu, Kulkarni, Misra, and Das (2007) |
| Distilled water | $TiO_2$ (20) | 0.024–1.18 | Ultrasonic bath | He et al. (2007) |
| R113 | CNTs | 0.2–1.0 | Ultrasonic bath | Jiang, Ding, and Peng (2009) |
| R113 | Cu, Ni, Al, CuO, $Al_2O_3$ | 0.1–1.2 | Ultrasonic bath | Jiang, Ding, Peng, Gao, and Wang (2009) |
| Distilled water | $CaCO_3$ (20–50) | 0.12–4.11 | Ultrasonic bath | Zhu, Li, Wu, Zhang, and Yin (2010) |
| Ethylene glycol –water (60:40) | CuO (30), $Al_2O_3$ (45), $SiO_2$ (50) | 0–6.12 | Ultrasonic bath | Kulkarni, Das, and Vajjha (2009) |
| Water, ethylene glycol | $Al_2O_3$ (50) | 0.5–6 | Ultrasonic bath | Anoop, Kabelac, Sundararajan, and Das (2009) |
| Ethylene glycol | $TiO_2$ (25) | 0–8 wt.% | Ultrasonic bath | Chen, Ding, He, and Tan (2007) |
| Ethylene glycol | $TiO_2$ (25) | 0.1–1.86 | Ultrasonic bath | Chen, Ding, and Tan (2007) |
| Ethylene glycol | TNT (~10), $L = 100$ nm | 0–8 wt.% | Ultrasonic bath | Chen, Ding, Lapkin, and Fan (2009) |
| Distilled water | CNT | 0.1–0.5 wt. % | Ultrasonic bath | Ding, Alias, Wen, and Williams (2006) |
| Ethylene glycol | CuO (12) | 0.002 | Ultrasonic bath | Kwak and Kim (2005) |
| Water | MWCNTs (20–30), $L = 10–30$ μm | 0.24–1.43 | Ultrasonic probe | Phuoc, Massoudi, and Chen (2011) |
| Water | MWCNTs (10–20) | 1 wt.% | Ultrasonic probe | Garg et al. (2009) |

(*Continued*)

**Table 2-2** (Continued)

| Base Fluid | Nanoparticle (dia. in nm) | Volume (%) | Synthesis Process | References |
|---|---|---|---|---|
| Car engine coolant | $Al_2O_3$ (<50) | 0.1–1.5 | Ultrasonic probe | Kole and Dey (2010) |
| Deionized water | $TiO_2$ (21) | 0.2–3 | Ultrasonic probe | Turgut et al. (2009) |
| Engine oil, ethylene glycol | Al (80) | 1–3 | Ultrasonic probe | Murshed, Leong, and Yang (2008) |
| Ethylene glycol –water (60:40) | $SiO_2$ (20, 50, and 100) | 0–10 | No information | Namburu, Kulkarni, Dandekar, and Das (2007) |
| Deionized water, ethylene glycol | $Al_2O_3$ (45) | 1–4 | Ultrasonic cleaner | Oh, Jain, Eaton, Goodson, and Lee (2008) |
| Water | $Al_2O_3$ (45) | 0.8 | Ultrasonic vibration | Patel et al. (2005) |

### 2.3.1 Ultrasonic Sonicator

From Table 2-2, it is clear that most of researchers used an ultrasonication process for proper dispersion of nanoparticles. Different ultrasonication processes have been used to stabilize nanoparticles in base fluids. Even though ultrasonication methods are popular among researchers, nevertheless, there is no standard procedure for the ultrasonication process to prepare nanofluids (specifically, types of ultrasonic processor and duration of sonication). Taurozzi, Hackley, and Wiesner (2012) report that an ultrasonic bath is not suitable for the dispersion of dry powders. However, it can be seen in Table 2-2 that many researchers are using ultrasonic baths for nanofluid preparation. Also, there are no standard guidelines about the percentage of amplitude and pulse on–off duration. Most researchers have ignored the ultrasonication duration, sonicator types, amplitudes, and the sequence of pulses as they do not mention this information in their papers (Elias et al., 2014; Murshed et al., 2008; Murshed, Tan, & Nguyen, 2008; Sohel et al., 2014; Turgut et al., 2009).

Based on the principle and types of ultrasonic machine, the process could be classified as direct and indirect ultrasonication. In general, an ultrasonic probe or horn is considered as a direct type, which is directly immersed into a mixture. An ultrasonic bath or cleaner type is considered as indirect sonication because the samples are kept inside a container and the container is submerged into the bath with liquid and ultrasonic waves are transmitted to the sample through the liquid in the bath (Taurozzi et al., 2012). Fig. 2-6 shows an illustrated example of direct and indirect sonication. Indirect sonication is not suitable for the dispersion of dry powders, and is not effective for high viscous fluid-based nanofluids. Therefore, an ultrasonic probe or "horn" is more effective for nanofluid preparation (Chung et al., 2009; Taurozzi et al., 2012).

Deciding on the proper sonication technique is of critical importance. For example, in Sharifalhoseini, Entezari, and Jalal (2015), direct (ultrasonic horn) and indirect sonication

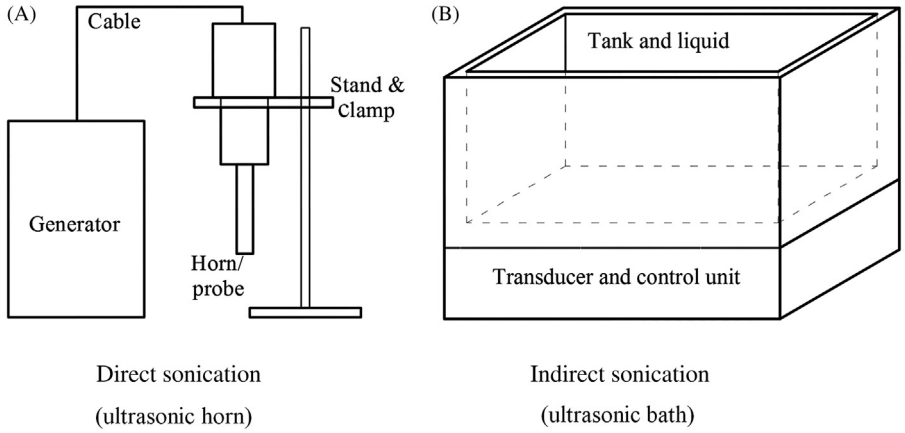


**FIGURE 2-6** Schematic example of (A) direct sonication and (B) indirect sonication.

(ultrasonic bath) were used during the preparation of ZnO nanofluids, and samples of ultrasonicated via direct and indirect methods were different from each other from a morphological point of view (Mahbubul et al., 2017). Here, a detailed example of a nanofluid preparation method using ultrasonic probe is explained. The nanofluid preparation procedure followed here was presented in previous works (Mahbubul et al., 2014, 2015a, 2015b, 2016a, 2016b), which were concerned with $Al_2O_3-H_2O$ nanofluid. No surfactants were added during the sample preparation. A flowchart elaborating the sample preparation procedure is given in Fig. 2-7. The experimental procedure for the preparation of nanofluids includes the following steps: weighing the desired amount of nanoparticle, $m_n$ and putting it into a vessel; in the next step adding the required amount of fluid, $m_l$ into that vessel. A precision analytical balance (GR-200, AND, Japan) was used to measure the weight of nanoparticles. This equipment has an accuracy of $\pm 0.0001$ g. The precision of nanoparticle weight and water volume were maintained as $\pm 0.001$ g and $\pm 0.5$ mL, respectively. [This paragraph is adapted from Mahbubul et al. (2017), copyright (2017), with permission from Elsevier.]

The following equation was used to determine the volume concentration of nanofluids:

$$\phi = \frac{m_n/\rho_n}{m_n/\rho_n + m_l/\rho_l} \tag{2.7}$$

where, $\phi$ is the particle volume fraction (vol.%); $m_n$ and $m_l$ are the mass of nanoparticle and the base fluid, respectively; and $\rho_n$ and $\rho_l$ are the density of nanoparticle and base fluid, respectively.

The type of ultrasonication discussed here is referred to as "direct sonication" (Taurozzi et al., 2012). As indicated in Taurozzi et al. (2012), direct sonication was advised over indirect sonication (done with ultrasonic baths), for dispersing dry powders within base fluids. The power of the device had 500 W, with an effective output of 282 W. The nanofluid samples with a nanoparticle fraction of 0.5% ($\phi$ = 0.5 vol.%) were prepared with ultrasonication

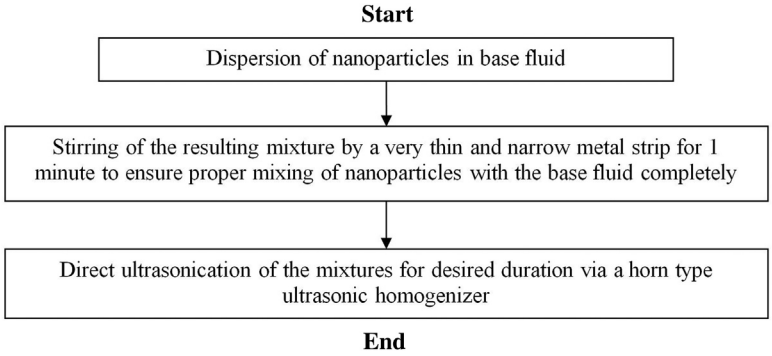


**FIGURE 2-7** Flowchart of nanofluid preparation by direct ultrasonication. *Adapted from Mahbubul, I.M., Elcioglu, E.B., Saidur, R., and Amalina, M.A. (2017). Optimization of ultrasonication period for better dispersion and stability of $TiO_2$–water nanofluid. Ultrasonics Sonochemistry 37, 360–367, copyright (2017), with permission from Elsevier.*

(amplitude: 50%, with 2 s ON and 2 s OFF pulses). Pulsed ultrasonication is generally advised since it impedes the temperature increase rate of the ultrasonicated material, minimalizes undesirable outcomes, and allows better temperature control in comparison to the continuous mode (Taurozzi et al., 2012). As a vital operation in the sample preparation, ultrasonication conceivably may have an impact on the total volume and the concentration of nanofluids, since the temperature of the ultrasonicated sample increases with agitation by 10°C/min, initially (Chung et al., 2009). A detail discussion of temperature generation is given in Subsection 2.3.1.1 (bulk heat analysis). To avoid this negative outcome, a digital refrigerated circulator bath (Model C-DRC 8, CPT Inc., South Korea) used for temperature control was connected with a recursion beaker, inside which the nanofluids were prepared at 15°C to avoid any possible vaporization of the base fluid. [This paragraph is adapted from Mahbubul et al. (2017), copyright (2017), with permission from Elsevier.]

The nanofluid preparation process is depicted in Fig. 2-8 as a schematic diagram, and in Fig. 2-9 as a pictorial representation. The following standard sizes (25, 50, 100, and 250 mL) of beakers were used to prepare 25, 50, 100, and 200 mL of nanofluid (when required in a single running/operation of the homogenizer), respectively, to receive maximum shear from the device. At least 2 cm of homogenizer horn was submerged in liquid and 1 cm clearance was maintained in between the tip end and the beaker inside bottom surface. The energy values corresponding to the ultrasonication durations (to study the effect of the duration for ultrasonication on nanofluid stability and other properties) are tabulated in Table 2-3.

### *2.3.1.1 Bulk Heat Analysis*

Before starting of the nanofluid preparation, it is necessary to be aware of the heat generation into the liquid due to ultrasonication. Fig. 2-10 shows the effect of evaporation during the ultrasonication process. Fig. 2-10A shows when the beaker is filled with 1 volume concentration (%) of $TiO_2$/R141b, just before starting the ultrasonication process. From Fig. 2-10A, it is clear that the level of liquid and solid mixture is greater than 80 mL.

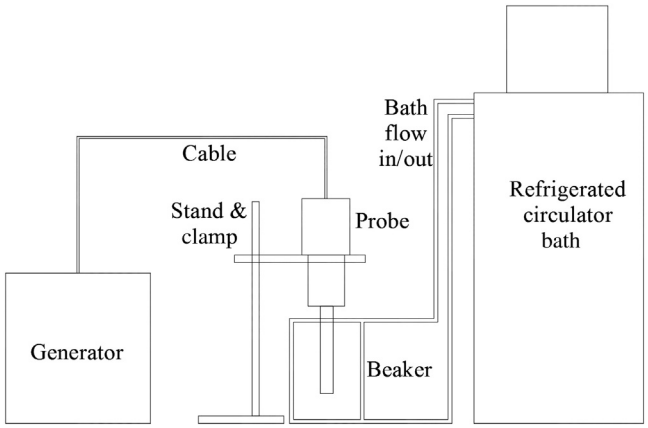


**FIGURE 2-8** Representation of nanofluid preparation setup by using an ultrasonic probe.

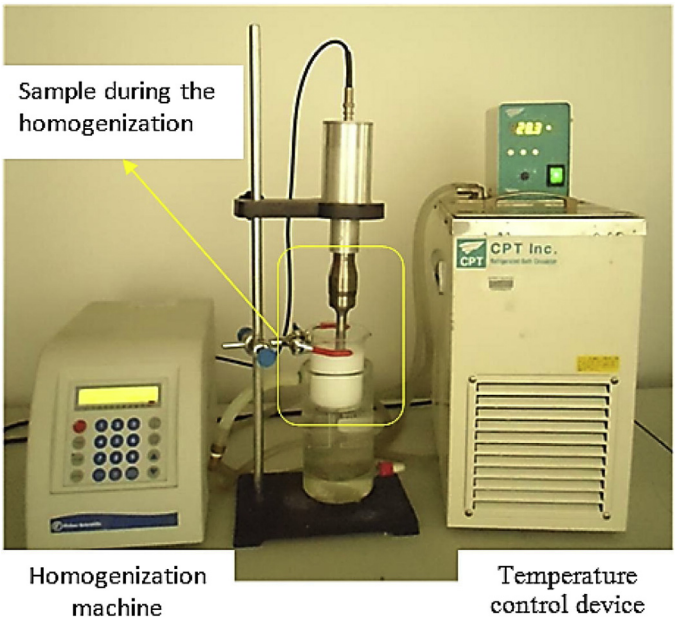


**FIGURE 2-9** Picture of nanofluid preparation setup. *Adapted from Mahbubul, I. M., Saidur, R., Hepbasli, A., and Amalina, M. A. (2016). Experimental investigation of the relation between yield stress and ultrasonication period of nanofluid.* International Journal of Heat and Mass Transfer 93*, 1169–1174, copyright (2015), with permission from Elsevier.*

Fig. 2-10B shows the level of the mixture is almost 40 mL after 30 min of ultrasonication. Therefore, about half of the liquid is evaporated due to the heat generated by the ultrasonication. Fig. 2-10C shows that the remaining amount is about 30 mL after 1 h of ultrasonication, which is the solid particles because most of the liquid is vaporized.

The rate of heat generation by ultrasonication was studied. To study the effect of bulk heating of the liquid, the horn (tip) ultrasonic dismembrator machine (Model 505, Fisher

**Table 2-3** Sonication Energy for Different Durations

| Duration (h) | Sonication Energy (J) |
|---|---|
| 1 | 8460 |
| 2 | 16,920 |
| 3 | 25,380 |
| 4 | 33,840 |
| 5 | 42,300 |

*Source*: Adapted from Mahbubul, I. M., Saidur, R., Hepbasli, A., and Amalina, M. A. (2016). Experimental investigation of the relation between yield stress and ultrasonication period of nanofluid. International Journal of Heat and Mass Transfer 93, 1169–1174, copyright (2015), with permission from Elsevier.

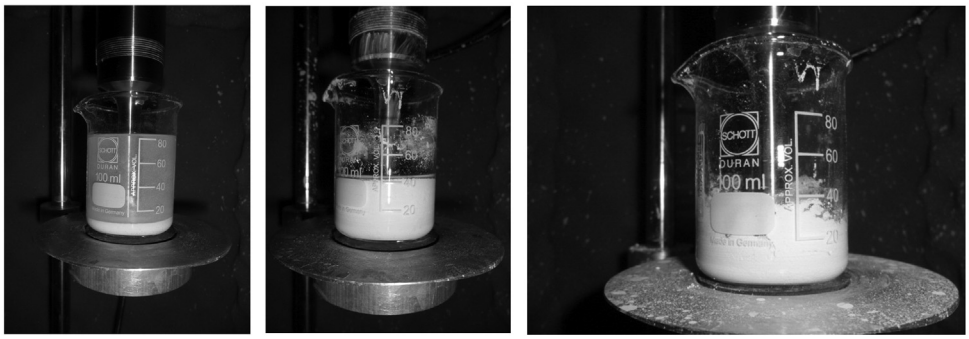


(A) (B) (C)

**FIGURE 2-10** Effect of evaporation during ultrasonication of $TiO_2$/R141b nanofluid: (A) before ultrasonication; (B) just after 30 min of ultrasonication; and (C) after 60 min of ultrasonication. *Reprinted with permission from Mahbubul, I. M. (2015). Investigation of fundamental properties of nanorefrigerants. LAP Lambert Academic Publishing, Saarbrücken, copyright (2015), OmniScriptum GmbH & Co. KG.*

Scientific, USA) was operated continuously for 5 min in four different volumes of distilled water—25, 50, 100, and 200 mL—with 50% amplitude (as for the ½-inch standard tip, this is the highest recommended % of amplitude), and continuous pulse mode. The capacity of the machine is designed as 20 kHz operating frequency and 500 W maximum input power. It should be noted that the 25, 50, 100, and 200 mL of water were filled in 50, 50, 100, and 250 mL standard beakers, respectively. For all the cases, a new sample was operating after the sonicator probe became normal (room temperature). At least 2.5 cm of the sonicator tip was immersed (from the top surface of the water level) into the water and at least 1 cm clearance between the beaker inner surface (bottom) and tip end surface was maintained. A temperature probe (with a capacity of $-100$ to 300°C with an accuracy of $\pm 1.0$°C) was immersed in the water and the data recorded on a computer.

The effect of ultrasonication in bulk heating of liquid is shown in Fig. 2-11. The y-axis values of the graph are the temperature differences, which were calculated by subtracting the measured temperature from the initial liquid temperature (room temperature). It can be seen from Fig. 2-11 that the influence of ultrasonication was more effective for lower liquid volumes. The temperature was increased with an increase in the sonication time and the increment

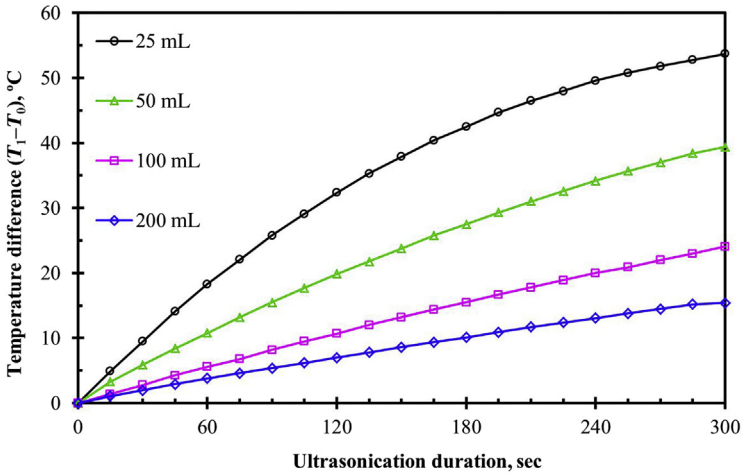


**FIGURE 2-11** Effect of ultrasonication in bulk heating of liquid.

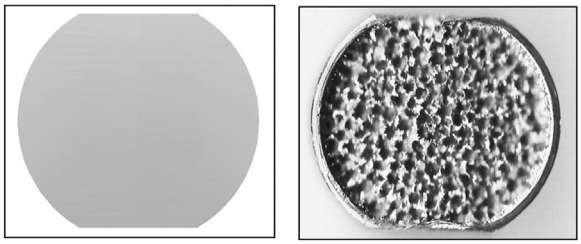


**FIGURE 2-12** Example of ultrasound tip erosion.

rates were found to be higher for a lower amount of water. After the first minute of ultrasonication, the increment rate was observed at 18.3, 10.8, 5.6, and 3.8°C for the liquid volume of 25, 50, 100, and 200 mL, respectively. Therefore, it is necessary to use a thermal bath or ice bath to control the temperature rise during the ultrasonication process. Otherwise, nanofluid will be evaporated and total volume and concentration will be changed. Chung et al. (2009) observed that agitation by ultrasonic horn increased the temperature by 10°C/min initially. Furthermore, they report that this increment rate was 1°C/min in an ultrasonic bath. They used 20 mL of deionized water to study the effect of ultrasonication on the temperature rise.

### *2.3.1.2 Tip Maintenance*

Maintenance of an ultrasound tip is necessary, whether it is a replaceable or continuous type. Over their lifetime, tips are eroded and reduce the performance of an ultrasonic homogenizer. Nevertheless, the erosion of a tip is an inescapable side effect of ultrasonication (Taurozzi et al., 2012). The examples of the end surface of a ½-inch new tip and worn tip is shown in Fig. 2-12A and B, respectively. The bottom surface of the tip of an ultrasonic

homogenizer that is required to be inspected before use every time. Based on the manufacturer guidelines, worn tips should be reconstructed.

## 2.3.2 High-Pressure Homogenizer

Fig. 2-13 shows a schematic illustration of the high-pressure homogenizer used in Hwang et al. (2008). It consists of two microchannels, dividing a liquid stream into two streams. Both liquid streams were divided and then recombined in a reacting chamber. Here the significant increase in the velocity of pressurized liquid streams in the microchannels resulted in the formation of cavitations in the liquid (Shaw, 1980). The high energy of cavitations was used to break the clusters of nanoparticles (Munson, Young, & Okiishi, 1998); where the nanoparticle suspension flows through a tube with the inner diameter of 3 mm prior to the interaction chamber in the high-pressure homogenizer. When the suspension reached inside the interaction chamber, it was designed to flow through the microchannel with an inner diameter of 75 μm. In such a contracting flow condition, the flow velocity of the suspension flowing through the microchannel should be increased up to ~1600 times according to Bernoulli's theorem, and simultaneously cavitation phenomena significantly occur. In this fast-flow region, particle clusters must be broken by the combination of various mechanisms, including (1) strong and irregular impaction on the wall inside the interaction chamber,

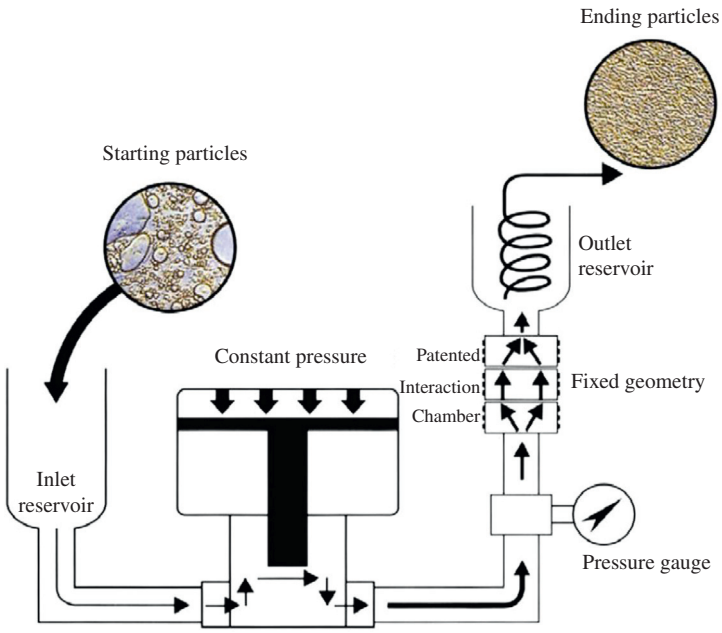


**FIGURE 2-13** Schematic diagram of the high-pressure homogenizer for producing nanofluids. *Reprinted from Hwang, Y., Lee, J.-K., Lee, J.-K., Jeong, Y.-M., Cheong, S.-I., Ahn, Y.-C., and Kim, S.H. (2008). Production and dispersion stability of nanoparticles in nanofluids. Powder Technology 186, 145–153, copyright (2007), with permission from Elsevier.*

(2) microbubbles formed by cavitation-induced exploding energy, and (3) high shear rate of flow. This leads to finally obtaining very homogeneous suspensions with less aggregated particles. Carbon black (CB)−water and Ag−silicon oil nanofluids were produced at the applied pressure of 18,000 psi, and then the nanofluids were passed through a high-pressure homogenizer three times to obtain sufficiently homogeneous nanoparticle distribution in the base fluids. As the results show (Figs. 2-20E and 2-21E), the particle clusters have been broken into the size of the primary particle size after three pass treatment at a pressure of 18,000 psi. [This paragraph is adapted from Hwang et al. (2008), copyright (2007), with permission from Elsevier.]

### 2.3.3 Mechanical Stirrer

A mechanical stirrer is also known as an overhead stirrer. This type of device is mostly used for mixing large volumes of liquids, with the liquid amount depending on motor power, speed, liquid viscosity, and many other factors. For effective mixing, several blades with different types, shapes, and sizes are attached to the shaft. Mahendran, Lee, Sharma, Shahrani, and Bakar (2012) prepared $TiO_2$−water nanofluid using a mechanical stirrer as shown in Fig. 2-14. The stirrer was operated for 2 h to get better homogeneous dispersion. Hwang et al. (2008) also used a stirrer to prepare CB−water and Ag−silicon oil nanofluids for comparison of the different two-step methods.

### 2.3.4 Shaker

The above examples (Sections 2.3.1−2.3.3) of nanofluid preparation are suitable for samples, which are liquid at atmospheric conditions. There are some fluids, like refrigerants, which also have the potential to be mixed with nanoparticles to enhance their cooling performance (Bi, Guo, Liu, & Wu, 2011; Mahbubul, Saadah, Saidur, Khairul, & Kamyar, 2015) but are not

(A) Stirred $TiO_2$ nanofluid (B) Prepared $TiO_2$ nanofluid

**FIGURE 2-14** Nanofluid preparation using a mechanical stirrer. *Reprinted with permission from Mahendran, M., Lee, G., Sharma, K., Shahrani, A., and Bakar, R. (2012). Performance of evacuated tube solar collector using water-based titanium oxide nanofluid. Journal of Mechanical Engineering and Sciences 3, 301−310, copyright: Universiti Malaysia Pahang, Pekan, Pahang, Malaysia.*

suitable to suspend nanoparticles using the above-discussed processing due to vaporization as shown in Fig. 2-10. The mixture of nanoparticles and refrigerant is called "nanorefrigerant." Presented here is an example of nanorefrigerant preparation methods. This method can be useful for samples, which are gaseous or low-temperature fluid. A nanorefrigerant can be managed inside an orbital incubator shaker, which must be closed and have a temperature control option. The incubator temperature needs to be maintained enough below the boiling point of the refrigerant to avoid vaporization. Such practice was used in Mahbubul (2015) and Mahbubul, Saidur, & Amalina (2013). However, better dispersion and stability could not be achieved by this process, as shown in Fig. 2-15. Nevertheless, three different samples ($Al_2O_3$/R141b nanorefrigerant, $Al_2O_3$/water, and $TiO_2$/water nanofluids) were prepared in Mahbubul (2015) and better stability was observed by checking a captured photograph using a digital camera. The prepared nanorefrigerant was kept in a closed glass bottle inside the normal chamber of a domestic refrigerator at below 15°C to avoid evaporation. The water-based nanofluids were kept inside an air-conditioned room (at room temperature). Fig. 2-16 shows the picture of 1 vol.% of $Al_2O_3$−R141b nanorefrigerant prepared by 24 h shaking with an orbital incubator shaker. The image of nanorefrigerants was taken until after 7 days of preparation with a time interval of 1 day (24 h). Fig. 2-16 shows that sedimentation starts after 4 days. The supernatant levels (empty spaces from the top) of the last four specimens imply sedimentation. The amounts of empty space on the top of the bottle "after 4 to 7 days" indicate that the sedimentation rate was very slow. Generally, the sedimentation of mixtures is measured from the bottom of the specimen. It could be possible when there are slurries obvious at the bottom of the sample. This happened especially for the low concentration in the suspension. The 1 vol.% of $Al_2O_3$−R141b nanorefrigerant considered

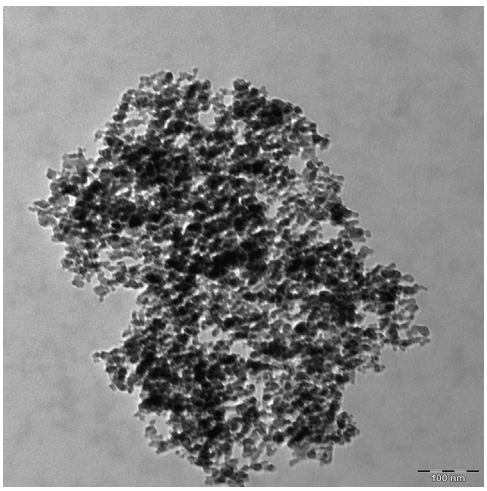


**FIGURE 2-15** TEM image of $Al_2O_3$−R141b nanorefrigerant prepared by using an incubator shaker. *Reprinted from Islam, M.M. (2012) Investigation of fundamental properties of nanorefrigerants. University of Malaya (Islam, 2012).*

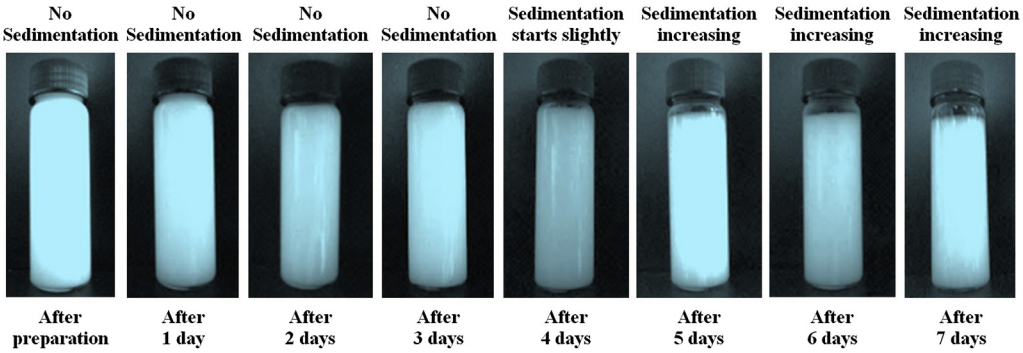


**FIGURE 2-16** Image of 1 vol.% of $Al_2O_3$−R141b nanorefrigerants started from just after the preparation to after 7 days of preparation with a time duration of 1 day (24 h). *Reprinted with permission from Mahbubul, I. M. (2015). Investigation of fundamental properties of nanorefrigerants. LAP Lambert Academic Publishing, Saarbrücken, copyright (2015), OmniScriptum GmbH & Co. KG, copyright (2015) OmniScriptum GmbH & Co. KG.*

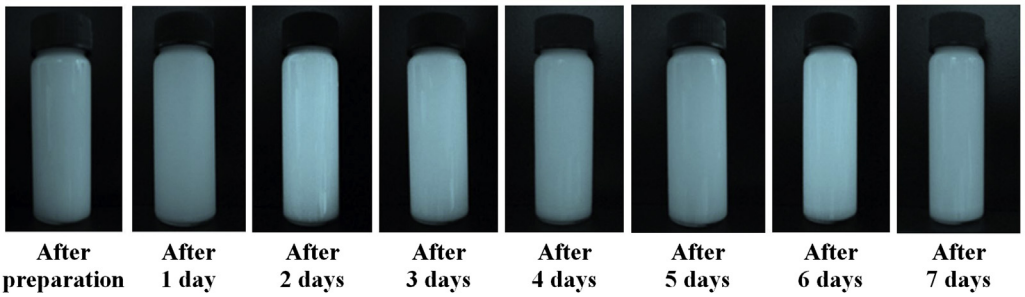


**FIGURE 2-17** Image of 1 vol.% of $Al_2O_3$−water nanofluid started from just after the preparation to after 7 days of preparation with a time duration of 1 day (24 h). *Reprinted with permission from Mahbubul, I. M. (2015). Investigation of fundamental properties of nanorefrigerants. LAP Lambert Academic Publishing, Saarbrücken, copyright (2015), OmniScriptum GmbH & Co. KG, copyright (2015) OmniScriptum GmbH & Co. KG.*

here is a moderate amount of volume fraction (neither too low nor too high a concentration) (Mahbubul, 2015).

Figs. 2-17 and 2-18 show 1 vol.% of $Al_2O_3$−water and $TiO_2$−water nanofluids, respectively, prepared by 24-h shaking with an orbital incubator shaker. The images show that there is no sedimentation until 7 days after preparation. In most cases, sedimentation depends on the viscosity of the base fluid as well as the preparation methods. The viscosity of water and R141b refrigerant are 0.85099 and 0.40021 mPa · s, respectively, at 27°C and at atmospheric condition (Lemmon, McLinden, & Huber, 2002). The higher viscosity of water could be a probable reason for the better stability observed for water-based nanofluids (Figs. 2-17 and 2-18) compared to R141b-based nanorefrigerant (Fig. 2-16). That's why the stability of ethylene glycol-based nanofluids is found to be better in comparison to water-based nanofluids (Ghadimi et al., 2011). Furthermore, water is a good solvent, having greater polarity, whereas refrigerants are not good solvents (nonpolar). Figs. 2-17 and 2-18 prove that nanofluids prepared by shaking have good stability (Mahbubul, 2015).

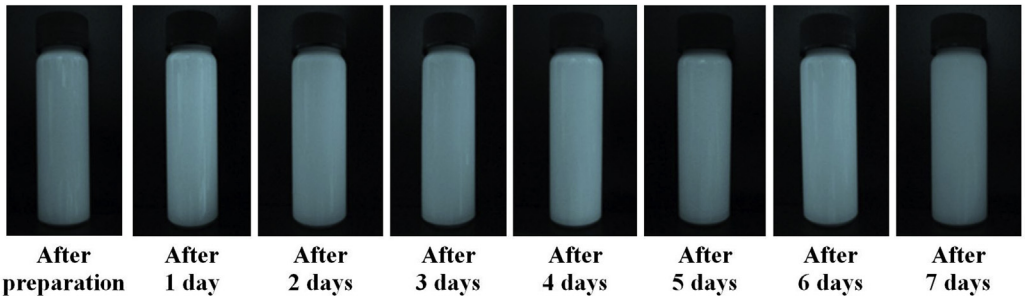


**FIGURE 2-18** Image of 1 vol.% of $TiO_2$–water nanofluid started from just after the preparation to after 7 days of preparation with a time duration of 1 day (24 h). *Reprinted with permission from Mahbubul, I. M. (2015). Investigation of fundamental properties of nanorefrigerants. LAP Lambert Academic Publishing, Saarbrücken, copyright (2015), OmniScriptum GmbH & Co. KG, copyright (2015) OmniScriptum GmbH & Co. KG.*

**Table 2-4** Processing Quantity of Different Two-step Methods

| Processor | Quantity That can be Processed at a Time |
|---|---|
| Ultrasonic homogenizer | 0.2–2000 mL |
| High-pressure homogenizer | 5–50 mL |
| Stirrer | Up to 200 L |
| Disperser | 0.5 mL–50 L |

## 2.3.5 Comparison of Two-Step Processes

Regardless of the quality, a general comparison is made in Table 2-4 regarding the processing quantity of some processors used in two-step methods. Table 2-4 states the range of a specific category. However, the specific processing capacity of a device will depend on its configuration and may differ from this chart.

Ghadimi and Metselaar (2013) studied the effect of different two-step homogenization techniques on the dispersion of $TiO_2$–distilled water nanofluid and average particle cluster size results are compiled in Table 2-5. Ultrasonic horn was found to be more effective based on the average particle cluster size. By using only 15 min of the ultrasonic horn, cluster size reduced to 188.2 nm, whereas it was 250.4 without any treatment and by using 3 h of an ultrasonic bath, it reduced to 212 nm only.

The quality of several two-step processing methods is compared in Hwang et al. (2008), where the effect of different mixture processes on the dispersion of silver (Ag)–silicon oil and carbon black (CB)–water nanofluids were studied. Fig. 2-19 shows a scanning electron microscopy (SEM) image of the tested nanoparticles (before being suspended in the base fluid). The images of Fig. 2-19 indicate that the nanoparticles were agglomerated. Fig. 2-20 shows the transmission electron microscopy (TEM) microstructures as dispersion status of Ag–silicon oil nanofluid prepared by (a) no physical treatment, (b) stirrer, (c) ultrasonic bath, (d) ultrasonic disruptor, and (e) high-pressure homogenizer. The stirrer used in the

**Table 2-5** Particle Cluster Size (average) of 0.1 wt.% $TiO_2$—water Nanofluid Prepared by Different Two-step Methods

| Homogenization Technique | Average Particle Cluster Size (nm) |
|---|---|
| Simple mixture | 250.4 |
| 15 min ultrasonic horn | 188.2 |
| 3 h ultrasonic bath | 212 |

*Source*: Adapted from Ghadimi, A., and Metselaar, I.H. (2013). The influence of surfactant and ultrasonic processing on improvement of stability, thermal conductivity and viscosity of titania nanofluid. Experimental Thermal and Fluid Science 51, 1—9, copyright (2013), with permission from Elsevier.

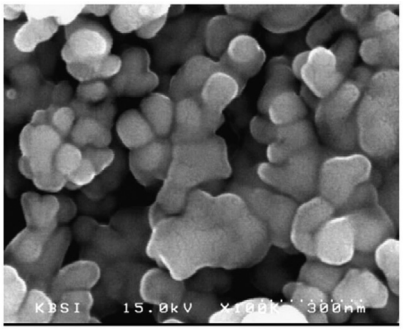


(A) Ag nanoparticles

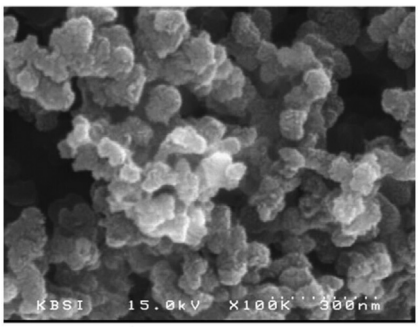


(B) CB nanoparticles

**FIGURE 2-19** SEM images of the tested nanoparticles. *Reprinted from Hwang, Y., Lee, J.-K., Lee, J.-K., Jeong, Y.-M., Cheong, S.-I., Ahn, Y.-C., and Kim, S.H. (2008). Production and dispersion stability of nanoparticles in nanofluids.* Powder Technology 186*, 145—153, copyright (2007), with permission from Elsevier.*

study had four blades. The revolution speed and operating time of blades were 1500 rpm and 2 h, respectively. The mixtures were sonicated for 1 h for both an ultrasonic bath (40 kHz) and an ultrasonic disruptor (20 kHz). The high-pressure homogenizer used in the study was M-110LCM, Microfluidics, Inc. (Hwang et al., 2008). More details of the high-pressure homogenizer in this study are described in Subsection 2.3.2. It can be seen in Fig. 2-20A that without any treatment, the Ag nanoparticles were in highly aggregated form

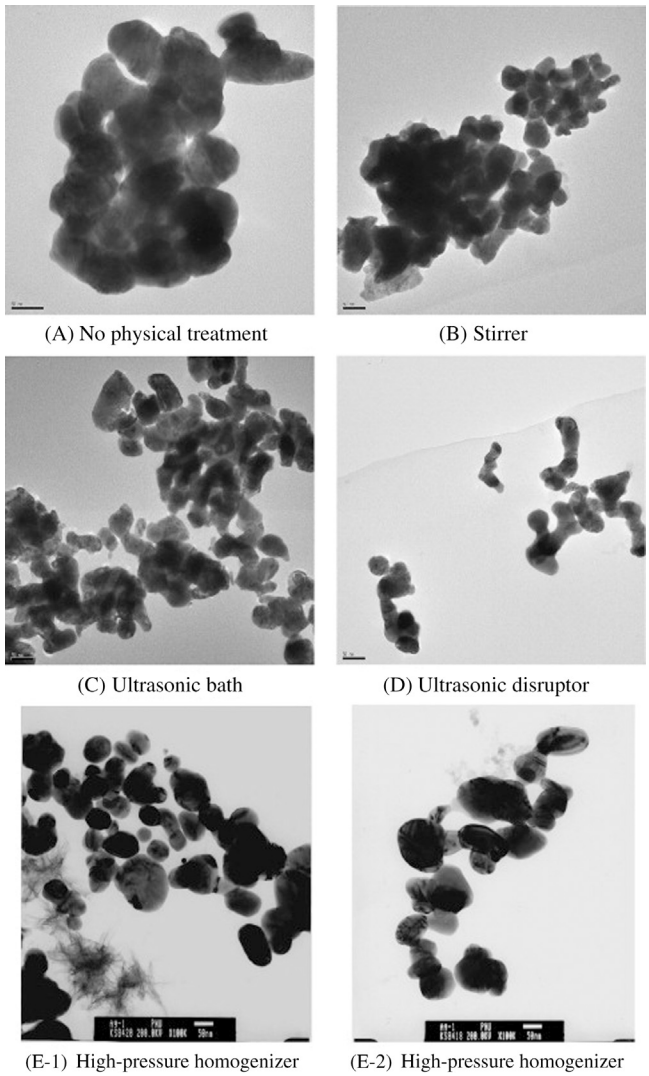


**FIGURE 2-20** TEM images of Ag particles in silicon oil-based nanofluids prepared by two-step methods (the inserted scale bar is 50 nm). *Reprinted from Hwang, Y., Lee, J.-K., Lee, J.-K., Jeong, Y.-M., Cheong, S.-I., Ahn, Y.-C., and Kim, S.H. (2008). Production and dispersion stability of nanoparticles in nanofluids.* Powder Technology 186, *145–153, copyright (2007), with permission from Elsevier.*

even with the presence of surfactants where the average diameter of the nanoparticle was 335 nm. Fig. 2-20B shows the image of a nanofluid prepared by a stirrer, indicating that it is not an effective way to avoid aggregation of particles. Fig. 2-20C and D show the microstructure of the nanofluid prepared by an ultrasonic bath and disruptor indicating better dispersion in comparison to Fig. 2-20A and B. However, the particle cluster in Fig. 2-20C is due to the lack of enough energy to break down the particle agglomeration. The images for a high-pressure homogenizer (Fig. 2-20E) are found to be better than others and the phenomenon

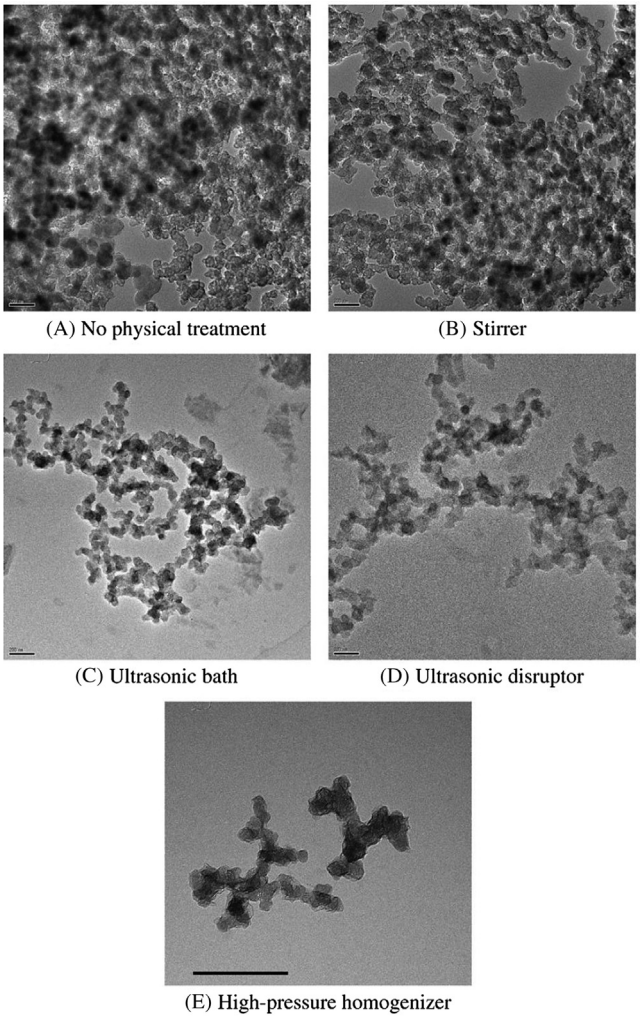


**FIGURE 2-21** TEM images of carbon black (CB) nanoparticles in water-based nanofluids prepared by two-step methods (the inserted scale bar is 200 nm). *Reprinted from Hwang, Y., Lee, J.-K., Lee, J.-K., Jeong, Y.-M., Cheong, S.-I., Ahn, Y.-C., and Kim, S.H. (2008). Production and dispersion stability of nanoparticles in nanofluids.* Powder Technology 186*, 145–153, copyright (2007), with permission from Elsevier.*

is discussed in Hwang et al. (2008). If a liquid mixture is passed into the interaction chamber (coated with diamond layer) of the microchannel then a cluster of particles tolerate too much impact. Due to that impact, silver particles were worn and rounded because the diamond coating layer is much harder than silver. Therefore, the morphology of Fig. 2-20E was a little different to the others (Hwang et al., 2008).

Fig. 2-21 shows the transmission electron microscopy (TEM) microstructures as dispersion status of CB–water nanofluid prepared by (a) no physical treatment, (b) stirrer,

(c) ultrasonic bath, (d) ultrasonic disruptor, and (e) high-pressure homogenizer. It can be seen in Fig. 2-21A that without any physical treatment, the nanoparticles were in a highly clustered form even with the presence of a surfactant. There was no significant change observed, even after using a stirrer as shown in Fig. 2-21B. Noticeable changes were observed after using an ultrasonic bath and disrupter (as shown in Fig. 2-21C and D). Aggregation size and the number of primary particles in a cluster were significantly decreased for the utilization of ultrasonication processes. Further, smaller particle clustering was observed in the morphology of nanofluid prepared by the high-pressure homogenizer (as shown in Fig. 2-21E) (Hwang et al., 2008).

Moreover, Hwang et al. (2008) studied the effect of different mixture processes on particle size distribution of (a) CB−water and (b) Ag−silicon nanofluids as shown in Fig. 2-22. The average diameter of the CB and Ag nanoparticle clusters were 585 and 335 nm, respectively, without any treatment. After using a stirrer, ultrasonic bath, ultrasonic disruptor, and high-pressure homogenizer, the average diameter of CB nanoparticle clusters were found to be 182, 147, 66, and 45 nm, respectively, which are 150, 90, 40, and 35 nm, respectively, in the case of Ag nanoparticles (Hwang et al., 2008). It could be concluded from Figs. 2-20−2-22 that a high-pressure homogenizer is the most effective method of nanofluid preparation. An ultrasonic disruptor (direct sonication) is also effective in dispersing nanoparticles in a liquid. Due to the high level of cost, bulky size and weight, and small amount of liquid processing, high-pressure homogenizers are not preferred by many researchers. On the other hand, ultrasonication processing is widely used because of its reasonable price, smaller size/features, and a substantial amount of liquid processing. More details about the effect of ultrasonication parameters on nanofluid stability and dispersion characteristics will be discussed in Chapter 3.

## 2.4 Comparison of One-Step and Two-Step Methods

Both types of nanofluid preparation methods have merits and demerits. It is well known that a large quantity of nanofluid can be prepared by the two-step method but the quality is poor. On the other hand, a high quality (in terms of stability) but comparatively lower quantity of nanofluid can be prepared by the one-step method.

Lee, Park, and Bang (2012) compared the dispersion and stability of 0.001 vol.% of CuO−deionized water (DIW) nanofluids prepared by one-step and two-step methods. They used Cu pellets to prepare CuO nanofluid by a one-step method of pulsed laser ablation in liquid where a single-pulsed laser beam was used and the process is as follows: (1) a beaker was filled with DIW and a copper pellet was placed at the bottom of it; (2) an Nd:YAG laser (LS-2134UTF model, made in Belarus LOTIS TII) was used for 8 h to synthesize CuO nanoparticle. The plasma state of Cu ion was produced by the targeted powerful energy over the copper pellet. In the two-step method, the CuO−DIW mixture was continuously sonicated for 6 h with PowerSonic 420 (Hwashin Technology Company, Korea). The TEM images of the nanofluids prepared by (a) the one-step method and (b) the two-step method as shown

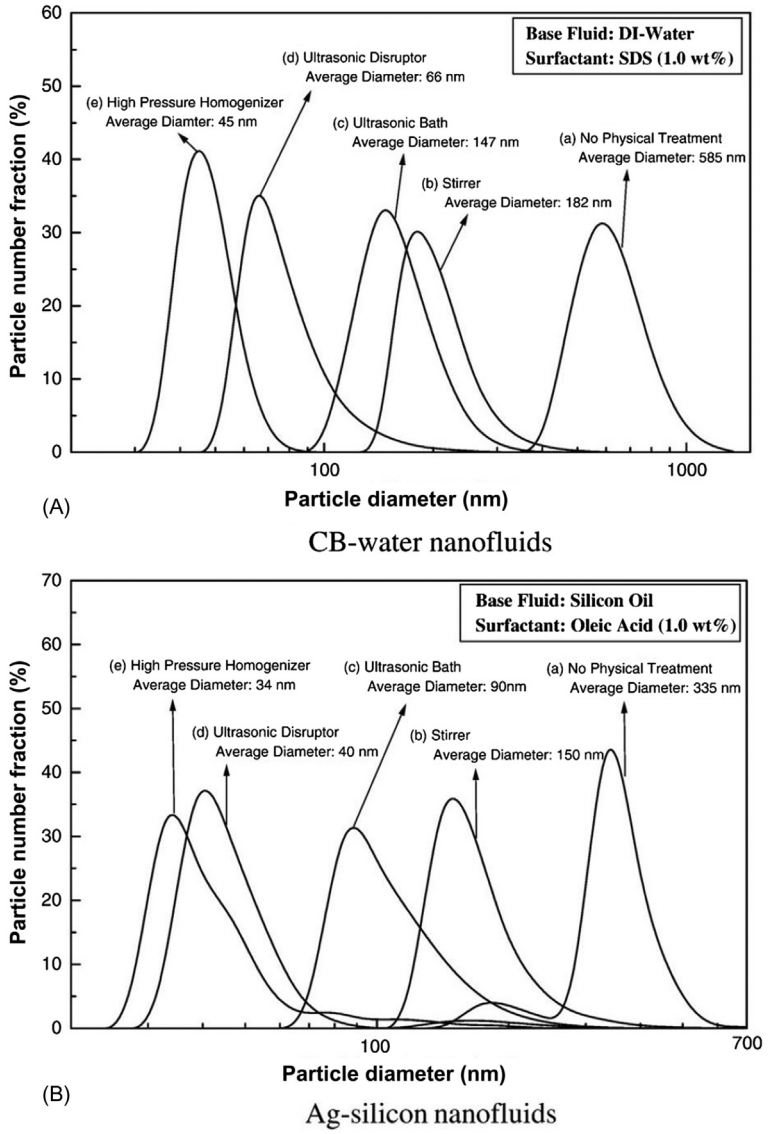


**FIGURE 2-22** The particle size distributions in nanofluids as a function of the dispersion methods. *Reprinted from Hwang, Y., Lee, J.-K., Lee, J.-K., Jeong, Y.-M., Cheong, S.-I., Ahn, Y.-C., and Kim, S.H. (2008). Production and dispersion stability of nanoparticles in nanofluids.* Powder Technology 186*, 145–153, copyright (2007), with permission from Elsevier.*

in Fig. 2-23. It can be seen in Fig. 2-23 that the sizes of CuO nanoparticles were smaller in (a) those prepared by the one-step method in comparison to (b) those prepared by the two-step method. The average sizes of nanoparticles were 15 and 55 nm in the one-step and two-step methods, respectively (Lee et al., 2012). Further, zeta potential and pH were measured

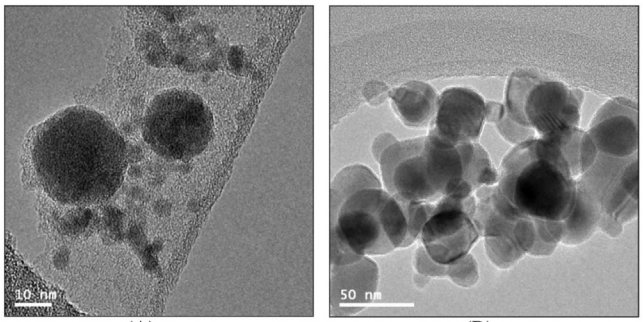


**FIGURE 2-23** TEM images of CuO nanoparticles according to manufacturing methods: (A) one-step method and (B) two-step method. *Reprinted from Lee, S.W., Park, S.D., and Bang, I.C. (2012). Critical heat flux for CuO nanofluid fabricated by pulsed laser ablation differentiating deposition characteristics.* International Journal of Heat and Mass Transfer 55*, 6908–6915, copyright (2012), with permission from Elsevier.*

**Table 2-6** Zeta Potential and pH of Two Nanofluids According to Manufacturing Method

| Properties | One-Step Method | Two-Step Method |
|---|---|---|
| Average particle size (nm) | 15 | 55 |
| Zeta potential | 39 | 15.8 |
| pH | 7.6 | 7.15 |

*Source*: Adapted from Lee, S.W., Park, S.D., and Bang, I.C. (2012). Critical heat flux for CuO nanofluid fabricated by pulsed laser ablation differentiating deposition characteristics. International Journal of Heat and Mass Transfer 55, 6908–6915, copyright (2012), with permission from Elsevier.

in Lee et al. (2012) to analyze the stability of the nanofluids, which are reported in Table 2-6. It was found that the stability of the nanofluid prepared by the one-step method was much higher than the nanofluid prepared by the two-step method.

# References

Akoh, H., Tsukasaki, Y., Yatsuya, S., & Tasaki, A. (1978). Magnetic properties of ferromagnetic ultrafine particles prepared by vacuum evaporation on running oil substrate. *Journal of Crystal Growth*, *45*, 495–500.

Anoop, K. B., Kabelac, S., Sundararajan, T., & Das, S. K. (2009). Rheological and flow characteristics of nanofluids: Influence of electroviscous effects and particle agglomeration. *Journal of Applied Physics*, *106*, 034909.

Bi, S., Guo, K., Liu, Z., & Wu, J. (2011). Performance of a domestic refrigerator using $TiO_2$-R600a nanorefrigerant as working fluid. *Energy Conversion and Management*, *52*, 733–737.

Chang, H., & Chang, Y.-C. (2008). Fabrication of $Al_2O_3$ nanofluid by a plasma arc nanoparticles synthesis system. *Journal of Materials Processing Technology*, *207*, 193–199.

Chang, H., Jwo, C. S., Fan, P. S., & Pai, S. H. (2007). Process optimization and material properties for nanofluid manufacturing. *The International Journal of Advanced Manufacturing Technology*, *34*, 300–306.

Chen, H., Ding, Y., He, Y., & Tan, C. (2007). Rheological behaviour of ethylene glycol based titania nanofluids. *Chemical Physics Letters*, *444*, 333–337.

Chen, H., Ding, Y., Lapkin, A., & Fan, X. (2009). Rheological behaviour of ethylene glycol-titanate nanotube nanofluids. *Journal of Nanoparticle Research*, *11*, 1513–1520.

Chen, H., Ding, Y., & Tan, C. (2007). Rheological behaviour of nanofluids. *New Journal of Physics*, *9*, 367.

Chevalier, J., Tillement, O., & Ayela, F. (2007). Rheological properties of nanofluids flowing through micro-channels. *Applied Physics Letters*, *91*, 233103.

Cho, T., Baek, I., Lee, J., & Park, S. (2005). Preparation of nanofluids containing suspended silver particles for enhancing fluid thermal conductivity of fludis. *Industrial & Engineering Chemistry Research*, *11*, 400–406.

Chung, S. J., Leonard, J. P., Nettleship, I., Lee, J. K., Soong, Y., Martello, D. V., & Chyu, M. K. (2009). Characterization of ZnO nanoparticle suspension in water: Effectiveness of ultrasonic dispersion. *Powder Technology*, *194*, 75–80.

Das, S., Choi, S., & Patel, H. (2006). Heat transfer in nanofluids—A review. *Heat Transfer Engineering*, *27*, 3–19.

Ding, Y., Alias, H., Wen, D., & Williams, R. A. (2006). Heat transfer of aqueous suspensions of carbon nanotubes (CNT nanofluids). *International Journal of Heat and Mass Transfer*, *49*, 240–250.

Eastman, J., Choi, S., Li, S., Yu, W., & Thompson, L. (2001). Anomalously increased effective thermal conductivities of ethylene glycol-based nanofluids containing copper nanoparticles. *Applied Physics Letters*, *78*, 718–720.

Elias, M. M., Mahbubul, I. M., Saidur, R., Sohel, M. R., Shahrul, I. M., Khaleduzzaman, S. S., & Sadeghipour, S. (2014). Experimental investigation on the thermo-physical properties of $Al_2O_3$ nanoparticles suspended in car radiator coolant. *International Communications in Heat and Mass Transfer*, *54*, 48–53.

Enustun, B. V., & Turkevich, J. (1963). Coagulation of colloidal gold. *Journal of the American Chemical Society*, *85*, 3317–3328.

Everett, D. H. (1988). *Basic principles of colloid science*. London: Royal Society of Chemistry.

Garg, J., Poudel, B., Chiesa, M., Gordon, J., Ma, J., Wang, J., … Nanda, J. (2008). Enhanced thermal conductivity and viscosity of copper nanoparticles in ethylene glycol nanofluid. *Journal of Applied Physics*, *103*, 074301.

Garg, P., Alvarado, J. L., Marsh, C., Carlson, T. A., Kessler, D. A., & Annamalai, K. (2009). An experimental study on the effect of ultrasonication on viscosity and heat transfer performance of multi-wall carbon nanotube-based aqueous nanofluids. *International Journal of Heat and Mass Transfer*, *52*, 5090–5101.

Ghadimi, A., & Metselaar, I. H. (2013). The influence of surfactant and ultrasonic processing on improvement of stability, thermal conductivity and viscosity of titania nanofluid. *Experimental Thermal and Fluid Science*, *51*, 1–9.

Ghadimi, A., Saidur, R., & Metselaar, H. S. C. (2011). A review of nanofluid stability properties and characterization in stationary conditions. *International Journal of Heat and Mass Transfer*, *54*, 4051–4068.

Goharshadi, E., Ding, Y., Jorabchi, M., & Nancarrow, P. (2009). Ultrasound-assisted green synthesis of nanocrystalline ZnO in the ionic liquid [hmim][NTf2]. *Ultrasonics Sonochemistry*, *16*, 120–123.

He, Y., Jin, Y., Chen, H., Ding, Y., Cang, D., & Lu, H. (2007). Heat transfer and flow behaviour of aqueous suspensions of $TiO_2$ nanoparticles (nanofluids) flowing upward through a vertical pipe. *International Journal of Heat and Mass Transfer*, *50*, 2272–2281.

Hiemenz, P. C., & Rajagopalan, R. (1997). *Principles of colloid and surface chemistry, Third edition, revised and expanded*. New York, NY: Marcel Dekker, Inc.

Hwang, Y., Lee, J.-K., Lee, J.-K., Jeong, Y.-M., Cheong, S.-I., Ahn, Y.-C., & Kim, S. H. (2008). Production and dispersion stability of nanoparticles in nanofluids. *Powder Technology*, *186*, 145–153.

Islam, M. M. (2012). *Investigation of fundamental properties of nanorefrigerants*. University of Malaya.

Jiang, W., Ding, G., & Peng, H. (2009). Measurement and model on thermal conductivities of carbon nanotube nanorefrigerants. *International Journal of Thermal Sciences*, *48*, 1108−1115.

Jiang, W., Ding, G., Peng, H., Gao, Y., & Wang, K. (2009). Experimental and model research on nanorefrigerant thermal conductivity. *HVAC&R Research*, *15*, 651−669.

Kole, M., & Dey, T. K. (2010). Viscosity of alumina nanoparticles dispersed in car engine coolant. *Experimental Thermal and Fluid Science*, *34*, 677−683.

Kulkarni, D. P., Das, D. K., & Vajjha, R. S. (2009). Application of nanofluids in heating buildings and reducing pollution. *Applied Energy*, *86*, 2566−2573.

Kumar, S. A., Meenakshi, K. S., Narashimhan, B. R. V., Srikanth, S., & Arthanareeswaran, G. (2009). Synthesis and characterization of copper nanofluid by a novel one-step method. *Materials Chemistry and Physics*, *113*, 57−62.

Kwak, K., & Kim, C. (2005). Viscosity and thermal conductivity of copper oxide nanofluid dispersed in ethylene glycol. *Korea-Australia Rheology Journal*, *17*, 35−40.

Lee, J., Hwang, K., Jang, S., Lee, B., Kim, J., Choi, S., & Choi, C. (2008). Effective viscosities and thermal conductivities of aqueous nanofluids containing low volume concentrations of $Al_2O_3$ nanoparticles. *International Journal of Heat and Mass Transfer*, *51*, 2651−2656.

Lee, S. W., Park, S. D., & Bang, I. C. (2012). Critical heat flux for CuO nanofluid fabricated by pulsed laser ablation differentiating deposition characteristics. *International Journal of Heat and Mass Transfer*, *55*, 6908−6915.

Lemmon, E. W., McLinden, M. O., & Huber, M. L. (2002). *NIST reference fluid thermodynamic and transport properties - REFPROP, version 7.0, NIST Standard Reference Database 23. "Database"*. Gaithersburg., Boulder: U.S. Department of Commerce.

Lo, C.-H., Tsung, T.-T., & Chen, L.-C. (2005). Shape-controlled synthesis of Cu-based nanofluid using submerged arc nanoparticle synthesis system (SANSS). *Journal of Crystal Growth*, *277*, 636−642.

Lo, C.-H., Tsung, T.-T., Chen, L.-C., Su, C.-H., & Lin, H.-M. (2005). Fabrication of copper oxide nanofluid using submerged arc nanoparticle synthesis system (SANSS). *Journal of Nanoparticle Research*, *7*, 313−320.

Mahbubul, I. M. (2015). *Investigation of fundamental properties of nanorefrigerants*. Saarbrücken: LAP Lambert Academic Publishing.

Mahbubul, I. M., Chong, T. H., Khaleduzzaman, S. S., Shahrul, I. M., Saidur, R., Long, B. D., & Amalina, M. A. (2014). Effect of ultrasonication duration on colloidal structure and viscosity of alumina−water nanofluid. *Industrial & Engineering Chemistry Research*, *53*, 6677−6684.

Mahbubul, I. M., Elcioglu, E. B., Saidur, R., & Amalina, M. A. (2017). Optimization of ultrasonication period for better dispersion and stability of $TiO_2$−water nanofluid. *Ultrasonics Sonochemistry*, *37*, 360−367.

Mahbubul, I. M., Saadah, A., Saidur, R., Khairul, M. A., & Kamyar, A. (2015). Thermal performance analysis of $Al_2O_3$/R-134a nanorefrigerant. *International Journal of Heat and Mass Transfer*, *85*, 1034−1040.

Mahbubul, I. M., Saidur, R., & Amalina, M. A. (2013). Influence of particle concentration and temperature on thermal conductivity and viscosity of $Al_2O_3$/R141b nanorefrigerant. *International Communications in Heat and Mass Transfer*, *43*, 100−104.

Mahbubul, I. M., Saidur, R., Amalina, M. A., Elcioglu, E. B., & Okutucu-Ozyurt, T. (2015a). Effective ultrasonication process for better colloidal dispersion of nanofluid. *Ultrasonics Sonochemistry*, *26*, 361−369.

Mahbubul, I. M., Shahrul, I. M., Khaleduzzaman, S. S., Saidur, R., Amalina, M. A., & Turgut, A. (2015b). Experimental investigation on effect of ultrasonication duration on colloidal dispersion and thermophysical properties of alumina−water nanofluid. *International Journal of Heat and Mass Transfer*, *88*, 73−81.

Mahbubul, I. M., Saidur, R., Amalina, M. A., & Niza, M. E. (2016a). Influence of ultrasonication duration on rheological properties of nanofluid: An experimental study with alumina−water nanofluid. *International Communications in Heat and Mass Transfer*, *76*, 33−40.

Mahbubul, I. M., Saidur, R., Hepbasli, A., & Amalina, M. A. (2016b). Experimental investigation of the relation between yield stress and ultrasonication period of nanofluid. *International Journal of Heat and Mass Transfer*, *93*, 1169−1174.

Mahendran, M., Lee, G., Sharma, K., Shahrani, A., & Bakar, R. (2012). Performance of evacuated tube solar collector using water-based titanium oxide nanofluid. *Journal of Mechanical Engineering and Sciences*, *3*, 301−310.

Mohammed, H. A., Al-aswadi, A. A., Shuaib, N. H., & Saidur, R. (2011). Convective heat transfer and fluid flow study over a step using nanofluids: A review. *Renewable and Sustainable Energy Reviews*, *15*, 2921−2939.

Munson, B. R., Young, D. F., & Okiishi, T. H. (1998). *Fundamentals of fluid mechanics* (3rd ed.). John Wiley & Sons.

Murshed, S., Leong, K., & Yang, C. (2008). Investigations of thermal conductivity and viscosity of nanofluids. *International Journal of Thermal Sciences*, *47*, 560−568.

Murshed, S. S., Tan, S.-H., & Nguyen, N.-T. (2008). Temperature dependence of interfacial properties and viscosity of nanofluids for droplet-based microfluidics. *Journal of Physics D: Applied Physics*, *41*, 085502.

Namburu, P., Kulkarni, D., Misra, D., & Das, D. (2007). Viscosity of copper oxide nanoparticles dispersed in ethylene glycol and water mixture. *Experimental Thermal and Fluid Science*, *32*, 397−402.

Namburu, P. K., Kulkarni, D. P., Dandekar, A., & Das, D. K. (2007). Experimental investigation of viscosity and specific heat of silicon dioxide nanofluids. *Micro & Nano Letters*, *2*, 67−71.

Oh, D., Jain, A., Eaton, J., Goodson, K., & Lee, J. (2008). Thermal conductivity measurement and sedimentation detection of aluminum oxide nanofluids by using the 3ω method. *International Journal of Heat and Fluid Flow*, *29*, 1456−1461.

Pak, B. C., & Cho, Y. I. (1998). Hydrodynamic and heat transfer study of dispersed fluids with submicron metallic oxide particles. *Experimental Heat Transfer*, *11*, 151−170.

Patel, H. E., Sundararajan, T., Pradeep, T., Dasgupta, A., Dasgupta, N., & Das, S. K. (2005). A micro-convection model for thermal conductivity of nanofluids. *Pramana*, *65*, 863−869.

Patungwasa, W., & Hodak, J. H. (2008). pH tunable morphology of the gold nanoparticles produced by citrate reduction. *Materials Chemistry and Physics*, *108*, 45−54.

Paul, G., Philip, J., Raj, B., Das, P. K., & Manna, I. (2011). Synthesis, characterization, and thermal property measurement of nano-Al95Zn05 dispersed nanofluid prepared by a two-step process. *International Journal of Heat and Mass Transfer*, *54*, 3783−3788.

Phuoc, T. X., Massoudi, M., & Chen, R.-H. (2011). Viscosity and thermal conductivity of nanofluids containing multi-walled carbon nanotubes stabilized by chitosan. *International Journal of Thermal Sciences*, *50*, 12−18.

Sharifalhoseini, Z., Entezari, M. H., & Jalal, R. (2015). Direct and indirect sonication affect differently the microstructure and the morphology of ZnO nanoparticles: Optical behavior and its antibacterial activity. *Ultrasonics Sonochemistry*, *27*, 466−473.

Shaw, D. J. (1980). *Introduction to colloid and surface chemistry*. London: Butterworths Press.

Sohel, M. R., Khaleduzzaman, S. S., Saidur, R., Hepbasli, A., Sabri, M. F. M., & Mahbubul, I. M. (2014). An experimental investigation of heat transfer enhancement of a minichannel heat sink using $Al_2O_3$−$H_2O$ nanofluid. *International Journal of Heat and Mass Transfer*, *74*, 164−172.

Taurozzi, J., Hackley, V., & Wiesner, M. (2012). *Preparation of nanoparticle dispersions from powdered material using ultrasonic disruption*. *NanoEHS protocols*. Gaithersburg, MD: National Institute of Standards and Technology.

Tseng, W. J., & Chen, C. N. (2003). Effect of polymeric dispersant on rheological behavior of nickel-terpineol suspensions. *Materials Science and Engineering A*, *347*, 145−153.

Tseng, W. J., & Lin, K. C. (2003). Rheology and colloidal structure of aqueous $TiO_2$ nanoparticle suspensions. *Materials Science and Engineering A*, *355*, 186−192.

Tseng, W. J., & Wu, C. H. (2002). Aggregation, rheology and electrophoretic packing structure of aqueous $Al_2O_3$ nanoparticle suspensions. *Acta Materialia*, *50*, 3757−3766.

Tsung, T.-T., Chang, H., Chen, L.-C., Liu, M.-K., Lin, H.-M., & Lin, C.-K. (2004). Process development of a novel arc spray nanoparticle synthesis system (ASNSS) for preparation of a $TiO_2$ nanoparticle suspension. *The International Journal of Advanced Manufacturing Technology*, *24*, 879−885.

Turgut, A., Tavman, I., Chirtoc, M., Schuchmann, H. P., Sauter, C., & Tavman, S. (2009). Thermal conductivity and viscosity measurements of water-based $TiO_2$ nanofluids. *International Journal of Thermophysics*, *30*, 1213−1226.

Wagener, M., Murty, B. S., & Günther, B. (1996). Preparation of metal nanosuspensions by high-pressure DC-sputtering on running liquids. *MRS Proceedings*, *457*, 149−154.

Wang, L., & Cheng, K. C. (1996). Flow transitions and combined free and forced convective heat transfer in rotating curved channels: The case of positive rotation. *Physics of Fluids*, *8*, 1553−1573.

Wang, L., & Liu, F. (2007). Forced convection in slightly curved microchannels. *International Journal of Heat and Mass Transfer*, *50*, 881−896.

Wang, L., & Yang, T. (2004). *Multiplicity and stability of convection in curved ducts: Review and progress*, . *Advances in Heat Transfer* (38, pp. 203−255). Elsevier.

Wang, X., Xu, X., & Choi, S. U. S. (1999). Thermal conductivity of nanoparticle-fluid mixture. *Journal of Thermophysics and Heat Transfer*, *13*, 474−480.

Wei, X., & Wang, L. (2010). Synthesis and thermal conductivity of microfluidic copper nanofluids. *Particuology*, *8*, 262−271.

Wei, X., Zhu, H., Kong, T., & Wang, L. (2009). Synthesis and thermal conductivity of $Cu_2O$ nanofluids. *International Journal of Heat and Mass Transfer*, *52*, 4371−4374.

Wen, D., & Ding, Y. (2005). Formulation of nanofluids for natural convective heat transfer applications. *International Journal of Heat and Fluid Flow*, *26*, 855−864.

Wu, D., Zhu, H., Wang, L., & Liua, L. (2009). Critical issues in nanofluids preparation, characterization and thermal conductivity. *Current Nanoscience*, *5*, 103−112.

Yu, W., Xie, H., Chen, L., Li, Y., & Zhang, C. (2009). Synthesis and characterization of monodispersed copper colloids in polar solvents. *Nanoscale Research Letters*, *4*, 465.

Yu, W., Xie, H., Li, Y., & Chen, L. (2011). Experimental investigation on thermal conductivity and viscosity of aluminum nitride nanofluid. *Particuology*, *9*, 187−191.

Zhu, H., Li, C., Wu, D., Zhang, C., & Yin, Y. (2010). Preparation, characterization, viscosity and thermal conductivity of $CaCO_3$ aqueous nanofluids. *Science China Technological Sciences*, *53*, 360−368.

Zhu, H.-T., Lin, Y.-S., & Yin, Y.-S. (2004). A novel one-step chemical method for preparation of copper nanofluids. *Journal of Colloid and Interface Science*, *277*, 100−103.